

Characterization of ^{99m}Tc-Resveratrol as a Cancer Targeting Radiopharmaceutical: An *In Vitro* study

Rozy Kamal¹, Vijayta D Chadha¹, Sohini Walia³ and Dhawan DK^{1,2*}

¹Centre for Nuclear Medicine, Panjab University Chandigarh-160014, India

²Department of Biophysics, Panjab University Chandigarh-160014, India

³Department of Microbiology, CSK, Himachal Pradesh Agricultural University, Palampur, India

*Corresponding author: Dhawan DK, Department of Biophysics, Panjab University, Chandigarh-160014, India, Tel: +91-172-2534121; E-mail: dhawan@pu.ac.in

Received date: December 22, 2015; Accepted date: February 08, 2016; Published date: February 12, 2016

Copyright: © 2016, Kamal R, et al. This is an open-access article distributed under the terms of the Creative Commons Attribution License, which permits unrestricted use, distribution, and reproduction in any medium, provided the original author and source are credited.

Abstract

Introduction: The present study describes the radio-synthesis, chemical characterization and bio-evaluation of ^{99m}Tc-resveratrol as a diagnostic imaging probe in radionuclide imaging of cancer using single photon emission computed tomography (SPECT).

Methods: Resveratrol, a potent chemopreventive natural phytoalexin was labeled with Technetium (^{99m}Tc). Radiolabeling efficiency, stability *in vitro*, cytotoxicity in rat RBCs and in HT29 colon cancer cells along with cellular internalization and binding characteristics were investigated.

Results: The radiochemical purity of synthesized radio-complex, ^{99m}Tc-resveratrol was >85%. ^{99m}Tc-resveratrol was stable upto 2 hours at room temperature between pH ranges 5-7. ^{99m}Tc-resveratrol, containing resveratrol up to a concentration of 20 μM was found to be nontoxic to both HT 29 cells and rat blood cells. Binding sites for ^{99m}Tc-resveratrol in HT 29 cells were found to be specific to native resveratrol and were concentrated in the cytosolic subcellular fraction of these cells. Cellular internalization of ^{99m}Tc-resveratrol was mainly through passive mode however active internalization via macropinocytosis was also observed.

Conclusion: The study, therefore reports the successful radio-synthesis of ^{99m}Tc-resveratrol complex, characterized as a stable, non-toxic and a potent cancer targeting probe.

Keywords: Resveratrol; Single photon emission computed tomography; HT 29; Cyclooxygenase-2; Radiopharmaceutical; Technetium; Cancer

Abbreviations:

PET: Positron Emission Tomography; SPECT: Single Photon Emission Computed Tomography; S.D.: Sprague Dawley; ^{99m}TcO₄⁻: Perchnetate; ERα: Estrogen Receptor Alpha; COX-2: Cyclooxygenase-2; ^{99m}Tc: Technetium-99m; MBq: Megabequerel; ^{99m}Tc-RH: Reduced/Hydrolyzed-^{99m}Tc; Rf: Retardation Factor

Introduction

Cancer diagnosis using radionuclide imaging has an edge over the anatomical imaging techniques, since these techniques can detect molecular changes in the tumor lesions. Such functional characterization of the tumor lesions can be accomplished with help of radionuclide-labelled radiotracers known as radiopharmaceuticals. However, efficacy of scintigraphic tumor imaging is extensively determined by the tumor specificity of radiopharmaceuticals. Thus, to improve the differential diagnosis, prognosis, planning and monitoring of cancer treatment, several functional pharmaceuticals have been developed and are being developed.

Resveratrol (3,4,5-trihydroxystilbene), is a natural phytoalexin found in grapes, berries and peanuts, and has wide applications in

cancer prevention and therapy. It can easily internalize cells and exhibits sensitivity and specificity for cancer cells while remaining non-toxic to normal cells [1]. Extensive *in vitro* studies have revealed that resveratrol, as a pharmacological agent, has a wide spectrum of targets in cancer cells [2]. The biological effectiveness of resveratrol in cancer therapy is thus a consequence of its simultaneous action on multiple molecular targets.

Resveratrol binds directly to the catalytic domain of cyclooxygenase-2 (COX-2) enzyme [3] which is found to be over expressed in several epithelial malignancies [4]. In normal cells however, COX-2 expression is induced only in the presence of cytokines, mitogens, and pro-inflammatory factors, which makes COX-2 a desirable molecular target to specifically target cancerous tissue using resveratrol.

Further, resveratrol has been characterized as a phytoestrogen based on its ability to compete with 17β-estradiol for binding to estrogen receptor alpha (ERα) [5-7]. Since enhanced ERα expression has been reported during advanced stages of colon cancer [8] and some other malignancies [9,10], recognition and differential binding of resveratrol to these receptor sites in cancerous and surrounding normal cells would give high target to nontarget binding uptake, which forms the basis of molecular imaging techniques like positron emission tomography (PET) and single photon emission computed tomography (SPECT). Using this principle, radiolabeled resveratrol is expected to

show localization in cancer cells by binding to single or multiple targets.

Despite numerous reports on cancer specificity of resveratrol in experimental and clinical research, use of this polyphenol as a radio imaging agent for cancer diagnosis is still unexplored. Therefore, with an aim to develop a SPECT based radiopharmaceutical with good sensitivity for cancer tissue, resveratrol in the present study was radiolabeled with ^{99m}Tc and further the binding characteristics of radiolabeled complex with HT 29 human colon cancer cell lines were evaluated *in vitro*.

Materials and Methods

Chemicals

HT 29 human colon cancer cell line was procured from National Centre for Cell Science (NCCS), Pune, India. McCoy's media [(supplemented with L-glutamine and sodium bicarbonate (NaHCO_3)), trans-resveratrol, n-octanol, stannous chloride dihydrate ($\text{SnCl}_2 \cdot 2\text{H}_2\text{O}$), (3-(4,5-Dimethylthiazol-2-yl)-2,5-diphenyltetrazolium bromide (MTT), cytochalasin B, colchicin, phenylarsine oxide, chlorpromazine, were purchased from Sigma-Aldrich (USA). Technetium-99m pertechnetate ($^{99m}\text{TcO}_4^-$) was procured from Post Graduate Institute of Medical Education and Research (PGIMER) Chandigarh, India. Instant thin layer chromatography-silica gel (ITLC-SG) strips were purchased from MERCK. Fetal bovine serum (FBS), trypsin-ethylene-diamine-tetra-acetic-acid (trypsin-EDTA), penicillin/streptomycin, and sodium pyruvate were purchased from Invitrogen (Carlsbad, CA). Trichloroacetic acid (TCA), sodium chloride (NaCl), hydrochloric acid (HCl), sodium di-hydrogen phosphate and disodium hydrogen phosphate were purchased from SRL. Fetal bovine serum (FBS), trypsin-ethylene-diamine-tetra-acetic-acid (trypsin-EDTA), penicillin/streptomycin, and sodium pyruvate were purchased from Invitrogen (Carlsbad, CA).

Cell culture

HT 29 cells were grown in McCoy's 5A media supplemented with L-glutamine, sodium bicarbonate, 10% FBS, 100 units/ml of penicillin, 100 $\mu\text{g}/\text{ml}$ of streptomycin and 1 mM sodium pyruvate. Cells were grown at 37°C in a humidified incubator with an atmosphere of 5% CO_2 and 95% air. Cells were passaged with 0.05% trypsin-EDTA solution after attaining 80% confluency, and cultures from the 3rd and 4th passage were used for cellular binding studies.

Radio-labeling and radio-chemical purity

^{99m}Tc -resveratrol was prepared by the addition of 3.7 Megabequerel (MBq) (100 μCi) of $^{99m}\text{TcO}_4^-$ to the reaction vial containing 100 μg (0.44 moles) of trans-resveratrol (2mg/ml solution in 10% ethanol) and 100 μg (0.44 moles) of $\text{SnCl}_2 \cdot 2\text{H}_2\text{O}$ [2 mg/ml solution in 0.1N HCl]. Total volume was made up to 0.7 ml with 0.9% saline to get a final concentration of 624 μM and 632 μM for resveratrol and $\text{SnCl}_2 \cdot 2\text{H}_2\text{O}$ respectively pH of the mixture was adjusted to 5-5.5 with 0.05 M NaHCO_3 . The reaction mixture was vortexed and kept at ambient temperature for sufficient time to complete the reaction. Labeling efficiency for ^{99m}Tc -resveratrol was evaluated by ascending chromatographic technique. Briefly, Whatman paper and ITLC-SG strips were cut into appropriate width and length (0.5 \times 10 cm) and were marked at the point of origin and end line (solvent front) from the base. A single spot of preparation was applied on the strip at the

point of origin. Strips were then placed in tubes containing different solvents to measure the amount of free $^{99m}\text{TcO}_4^-$, and reduced/hydrolyzed- ^{99m}Tc (^{99m}Tc -RH) fraction in the preparation. The strips were left undisturbed in the developing tubes to allow movement of the solvent and then removed after the solvent touched the end line. The strips were air dried, cut into 0.5 cm long sections and then counted for activity using well-type gamma-sensitive probe (ECIL, Hyderabad, India).

Paper electrophoresis

Paper electrophoresis was performed to determine the net charge on ^{99m}Tc -resveratrol and to separate different radiochemical moieties (free $^{99m}\text{TcO}_4^-$, ^{99m}Tc -RH, and ^{99m}Tc -resveratrol) formed during radio-synthesis of ^{99m}Tc -resveratrol, depending on their electrophoretic mobility. Free $^{99m}\text{TcO}_4^-$ and ^{99m}Tc -RH colloids were also run simultaneously as reference standards, along with the test formulation (^{99m}Tc -resveratrol) to determine the migration distances under similar experimental conditions. Electrophoresis was carried out at 300V for 40 min using phosphate buffer saline (0.05M; pH 6.80) as electrolytes source solution. After complete development, the Whatman paper was removed, dried, and cut into strips. Each strip measuring 0.5 cm, was then counted in a well type gamma counter. The results were expressed as percentage ratio of the radioactivity of the radiochemical specie to the total activity.

In vitro stability

In vitro stability of ^{99m}Tc -resveratrol preparation as a function of time was examined in order to determine the appropriate time for the radio-complex to be injected intravenously, before undesired products are formed that may alter the bio-distribution of the complex *in vivo*. Radiochemical purity of the radiocomplex was analysed at different time intervals for a period of 2 hours after addition of $^{99m}\text{TcO}_4^-$ to the reaction vial. Further, stability of the radio-complex at different pH was also examined.

Stability of the radio-complex in serum was determined by incubating 100 μl of the radio-complex (3.7MBq) with 900 μl of serum for different time intervals at 37°C . Blood was drawn from rats under light ether anesthesia by puncturing the retro-orbital plexus using sterilized glass capillaries. Samples were then kept for 2 hours at room temperature. Serum was separated after centrifuging the blood samples at 1500 rpm for 10-15 min. The serum samples were then assessed for any dissociated or degraded radio-complex at regular time intervals for a time span of 4 hours using paper chromatography.

Toxicity Studies

MTT assay

Cytotoxicity of ^{99m}Tc -resveratrol was evaluated in HT 29 cells, by using MTT (3-(4, 5-Dimethylthiazol-2-yl)-2, 5-diphenyltetrazolium bromide), a tetrazole assay as described by Mosmann, 1983 [11]. Approximately 1×10^5 cells were plated at a density of approximately 10^6 cells per well in 96-well tissue culture plates and were allowed to attach overnight at 37°C in humidified atmosphere with 5% CO_2 . The next day, fresh media containing different concentrations of ^{99m}Tc -resveratrol (2.5, 5, 10, 20, 30, 60, and 160 μM) was added to the plate in triplicates. After 24 hours of incubation, fresh media containing 5 μl (0.25 mg/ml) of MTT reagent was added to each well which was further incubated for 4 hours. Formazon crystals formed after 4 hours

in each well were dissolved in 150 µl of DMSO and the plates were read immediately in a microplate reader (BIO-RAD microplate reader-550) at 570 nm with reference wavelength of 690 nm. Wells containing cells incubated with 10% triton X 100 were treated as negative control and those containing assay medium without ^{99m}Tc-resveratrol were treated as positive control. Wells containing assay medium and MTT reagent, without cells were used as blanks. Cell viability at different concentrations of ^{99m}Tc-resveratrol was calculated in relation to positive control cells for which percentage viability was taken as 100%.

Cell viability (%)=(Absorbance of sample) × 100/(Absorbance of positive control)

Trypan blue exclusion assay

The dye exclusion test is used to determine the number of viable cells present in a cell suspension. Live cell membranes exclude certain dyes, such as trypan blue, eosin, or propidium, whereas dead cells do not. After incubating the cells (HT 29) with different concentration of ^{99m}Tc-resveratrol for 24 hours as described above for MTT assay, cells were removed from the wells and suspended in PBS. 100µl of trypan blue (0.4%) was added to 500 µl of cell suspension containing 10⁵ cells ml⁻¹. The cells were immediately loaded on a haemocytometer and were examined under a microscope. The number of blue staining cells and the number of total cells were counted in 6 different fields for each sample. Percentage viability was expressed in relation to control cells (containing assay medium without ^{99m}Tc-resveratrol) for which cell viability was taken as 100%.

Viable cell fraction (VF)=[1.00-(Number of blue cells ÷ Number of total cells)]

Cell viability (%)=(VF of sample) × 100/(VF of positive control)

Haemoglobin release assay

Blood haemolysis in the presence of test drugs is a fast, efficient, simple, and low-cost procedure to investigate the cytotoxicity of drugs on erythrocytes' membrane by spectrophotometric measurement of the released haemoglobin [12]. The amount of haemolysis i.e. absorbance values of released haemoglobin is directly proportional to the level of toxicity. The *in vitro* cytotoxic effect of ^{99m}Tc-resveratrol was studied by using heparinized venous blood samples collected from healthy rats. Fresh blood samples were centrifuged (4000 rpm for 5 min) at 4°C using a refrigerated centrifuge, and the plasma and buffy coat were carefully removed by aspiration. The red blood cells were washed three times by centrifugation (4000 rpm for 5 min) in cold phosphate buffer solution (0.15 mM NaCl, 50 mM NaH₂PO₄/Na₂HPO₄, pH=7.4) and were finally resuspended with the same buffer to obtain a hematocrit of 5%. Freshly prepared aqueous solutions containing different concentrations of ^{99m}Tc-resveratrol were added to 450 µl of 5% red blood cell suspension in triplicate and the final volume was made 500 µl with previously prepared phosphate buffer solution. The samples were then incubated at 37°C for 24 hours under constant shaking at 120 rpm. The red blood cell suspension was then centrifuged at 4000 rpm for 5 min. Haemolysis was determined by measuring the absorbance at 540 nm using a spectrophotometer (Shimadzu UV-visible spectrophotometer). 1% triton X was used as a positive control and PBS was used as a negative control (blank). Percentage haemolysis for different concentration of ^{99m}Tc-resveratrol was finally presented in relation to positive control (1% triton X 100) for which haemolysis percentage was taken as 100%.

Haemolysis by the test sample was calculated using the following equation.

Haemolysis (%)=(Absorbance of test sample) × 100/(Absorbance of positive control)

Total cell binding, internalization and sub-cellular fraction binding

The binding properties of a drug may vary with the incubation time and concentration of the drug incubated with the cells.

In order to study the binding characteristics of ^{99m}Tc-resveratrol, HT 29 human colon cancer cells were plated at a density of approximately 106 cells per well in 12-well tissue culture plates and was allowed to attach overnight at 37°C in humidified atmosphere with 5% CO₂. The following day, cells were incubated with different concentrations of the radio-complex for different time intervals upto 4 hours. At different time points over a period of 4 hours, incubation was terminated by washing the cells twice with ice-cold PBS. Cell surface bound radioactive complex was removed by two steps of acid wash (50 mM glycine HCl/100 mM NaCl, pH 2.8) at room temperature for 3 min. pH was neutralized with cold PBS with 0.2% bovine serum albumin (BSA) and, subsequently, the cells were lysed in 500 µl of lysis buffer (Tris 10 mM, MgCl₂ 3 mM, NaCl 10 mM, 0.1% triton X-100 pH 7.5-8.0). After 30 min of incubation in lysis buffer, the cell suspension was removed and centrifuged at 1300 g at 4°C for 5 min to pellet nuclei and cell debris (P1). The supernatant obtained (S1) was further centrifuged at 20,000 g at 4°C for 20 min to obtain free membrane and soluble cytosolic proteins as supernatant (S2) and large intact organelles as pellet (P2). At different incubation time, the unbound activity (activity outside the cell), cell surface bound activity and the activity associated to different subcellular fractions, (activity in the nucleus (P1), outside the nucleus (S1), free membranes and soluble proteins i.e. cytosol (S2) and large intact organelles (P2) were measured (at least 3 replicates) in a gamma-counter.

Total cell binding (sum of cell surface bound activity and the activity associated to different subcellular fractions) at different time points for different concentrations was expressed as the percentage fraction of total added activity. Cell internalization was expressed as the percentage fraction of total cell bound activity.

Saturation binding

Having determined the time for maximum binding, saturation binding characteristics for ^{99m}Tc-resveratrol were evaluated in different cellular fractions. Radio-labeled drugs may bind to specific binding sites, i.e. sites characteristic of the native unlabeled drug or it may bind to sites other than the specific sites, in which case the binding is said to be nonspecific. The binding affinity to the specific sites and the density of these sites is represented by binding parameters, viz. K_d (ligand concentration that binds to half the receptor sites at equilibrium) and β max (maximum number of binding sites) which are obtained from the saturation binding experiments. In these experiments, specific binding (total- nonspecific binding) is evaluated for a range of radio-ligand concentration and plotted graphically in a Scatchard plot. The plot is then used to evaluate the binding parameters, K_d and β max.

Two sets of triplicates of different ^{99m}Tc-resveratrol concentrations were prepared for total and non-specific binding studies. Each well of the first set containing 106 cells in assay medium was incubated with a different concentration of ^{99m}Tc-resveratrol (total binding) for 2 hours

at 37°C. For nonspecific binding, 100µM [13] of unlabelled resveratrol was added as a competitor to each well along with ^{99m}Tc -resveratrol and was incubated for 2 hours at 37°C. The radioactivity associated to each fraction at different concentrations of the radio-complex was recorded and expressed as counts per second (cps) per 10^6 cells. Graph Pad Prism 6.05 program (Graph Pad Software, San Diego, CA) was used for data analysis and for determining the binding parameters, K_d and β max.

Mechanism of Cell Internalization

Cell internalization can occur actively or passively. To account for passive internalization, cell internalization of ^{99m}Tc -resveratrol at different concentrations and for different time intervals were simultaneously carried out at 4°C along with 37°C as described above. Incubation at 4°C inhibits active processes, as several proteins and enzymes are sensitive to temperature [14,15], therefore, the uptake obtained at 4°C would correspond to passive uptake. To further explore the active process, internalization assay was performed at 37°C and 4°C, with and without endocytosis inhibitor (50 mM chlorpromazine), 25 µg/ml colchicine or 5 µg/ml cytochalasin B, inhibitors of pinocytosis, and macropinocytosis, respectively and 0.1% sodium azide to induce ATP depletion in order to inhibit energy dependent internalization. The cells were pretreated for 60 minutes in assay medium containing 25 µg/ml colchicines, 5 µg/ml cytochalasin B, 50 mM chlorpromazine, and 0.1% sodium azide. Following the removal of the pretreatment solution, the cells were washed with PBS, treated with 10 µM of ^{99m}Tc -resveratrol and incubated under the conditions used for cell culture. Cellular accumulation of ^{99m}Tc -resveratrol at 2 hours was measured. At the end of the incubation period, the media containing free ^{99m}Tc -resveratrol was removed and the cells were washed 3 times with cold PBS. Membrane integrity of cells treated with the inhibitors was confirmed by trypan blue exclusion assays to rule out disruption of membrane by different treatments. Cells were then lysed in a lysis buffer and radioactivity associated with cell lysates and media was measured. ^{99m}Tc -resveratrol uptakes by cells pretreated with endocytosis inhibitors were compared with those without pretreatment, and the reduction in ^{99m}Tc -resveratrol uptake caused by the inhibitors was calculated.

Statistical Analysis

Experiments were repeated at least 2 times, each time in triplicate. The binding parameters were determined using Graph Pad Prism program (version 6.05) (Graph Pad Software Inc., San Diego, CA, USA). Vehicle control group were compared with the treatment group unless otherwise specified. Significant intergroup differences were evaluated by using one-way ANOVA followed by Newman Keuls' multiple comparisons with p values ≤ 0.05 being considered as statistically significant. The statistical software package SPSS v 14.0 for windows was used for the purpose.

Results

Retardation factor

The retardation factor (Rf) values for the three radiochemical moieties present in the formulation viz. $^{99m}\text{TcO}_4^-$, ^{99m}Tc -RH and ^{99m}Tc -resveratrol were obtained using ascending chromatography technique (Table). Characteristic Rf value for each component present in the mixture was obtained by separating each component with

suitable combination of mobile and stationary phases. $^{99m}\text{TcO}_4^-$ revealed an Rf value of 1 with Whatman paper as stationary phase and acetone as mobile phase. However, Rf zero was obtained for ^{99m}Tc -RH using all the three solvents/solvent mixtures (solvent A-normal saline; solvent B-butanol: pyridine: water: glacial acetic acid in the ratio 30:20:20:6; solvent C- pyridine: water: acetic acid in the ratio 3:5:1.5) as mobile phase and silica coated ITLC strips as stationary phase. Maximum separation of ^{99m}Tc -resveratrol, from the other two undesired forms of ^{99m}Tc ($^{99m}\text{TcO}_4^-$ and ^{99m}Tc -RH) was obtained at Rf=0.7, by using solvent B as mobile phase and silica as stationary phase. Therefore, paper chromatography using acetone and ITLC using solvent B as mobile phases were used to assess the radiochemical purity of the compound during optimization of the chemical constituents and different reaction conditions required to obtain maximum yield of ^{99m}Tc -resveratrol.

Mobile phase		Acetone	Solvent A	Solvent B	Solvent C
Stationary phase		Paper	Silica	Silica	Silica
	^{99m}Tc -resveratrol	0.0	0.9 ± 0.1	0.7 ± 0.0	1 ± 0.0
	Pertechnetate	1 ± 0.0z	1 ± 0.0	1 ± 0.1y	1 ± 0.0
	Reduced/hydrolysed ^{99m}Tc	0.0	0.0z	0.0z	0.0z

Table 1: Retardation factor values of radio-chemical moieties in different sets of mobile and stationary phases.

Optimization of radiochemical yield

Optimization of $\text{SnCl}_2 \cdot 2\text{H}_2\text{O}$

Keeping the amount of $^{99m}\text{TcO}_4^-$ activity (3.7MBq) and the amount of resveratrol (624 µM) fixed, amount of $\text{SnCl}_2 \cdot 2\text{H}_2\text{O}$ was varied and the radiochemical yield of ^{99m}Tc -resveratrol was observed after 30 min of incubation at room temperature. As shown in Figure 1a, the labeling yield significantly increased with increase in the amount of $\text{SnCl}_2 \cdot 2\text{H}_2\text{O}$, whereby a maximum yield of $89.4 \pm 0.35\%$ was obtained at a concentration of 632 µM. Increasing the amount of $\text{SnCl}_2 \cdot 2\text{H}_2\text{O}$ beyond 632 µM decreased the labeling yield, as excess $\text{SnCl}_2 \cdot 2\text{H}_2\text{O}$ is known to form insoluble colloids that can co-precipitate with reduced $^{99m}\text{TcO}_4^-$ thereby reducing the labelling efficiency [16].

Optimization of resveratrol

The amount of resveratrol was varied keeping $^{99m}\text{TcO}_4^-$ activity (3.7 MBq) and the amount of $\text{SnCl}_2 \cdot 2\text{H}_2\text{O}$ (632 µM) and incubation time (30 min) fixed. As shown in Figure 1b, initially an increase in the radiochemical yield was observed with increase in resveratrol amount, since the number of resveratrol molecules available for binding with reduced technetium-99m molecules were also increasing. Maximum yield of $89.4 \pm 1\%$ was achieved with 624 µM of resveratrol but further increase in the amount of resveratrol decreased the labelling yield by increasing the colloidal fraction in the formulation.

Optimization of $^{99m}\text{TcO}_4^-$ activity

Altering the amount of $^{99m}\text{TcO}_4^-$ in the formulation also affected the labelling yield (Figure 1c) whereby both insufficient and excess amount

of $^{99m}\text{TcO}_4^-$ decreased labelling yield by increasing the amount of colloidal fraction in the formulation. The reason for colloid formation at low levels of $^{99m}\text{TcO}_4^-$ is unclear but excess of $^{99m}\text{TcO}_4^-$ in the absence of required amount of pharmaceutical is known to undergo hydrolysis in aqueous solution to forms colloids.

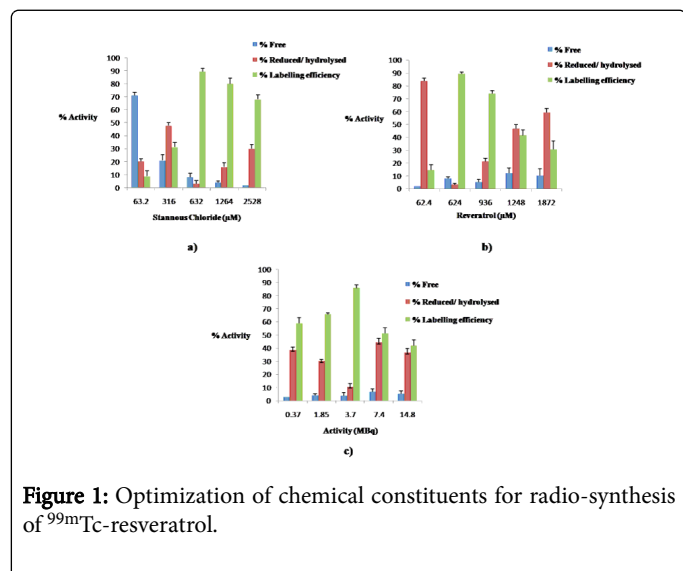


Figure 1: Optimization of chemical constituents for radio-synthesis of ^{99m}Tc -resveratrol.

Percentage radiolabeling efficiency with different amount of a) $\text{SnCl}_2 \cdot 2\text{H}_2\text{O}$ b) trans-resveratrol and c) $^{99m}\text{TcO}_4^-$ radioactivity was evaluated using ascending chromatography. Experiment was run with samples in triplicate and repeated 2 times.

Paper electrophoresis

Under the same experimental conditions, the migration distances travelled by ^{99m}Tc -complexes toward the anode on paper strips during electrophoresis were obtained and are shown in Figure 2. Four different peaks were obtained on the electro-phoretogram using ^{99m}Tc -resveratrol, depending on the electrophoretic mobility of chemical species present in preparation. The values for the distance (in cm) travelled by the complexes towards the anode were as follows: The first peak was obtained at 0 cm from the cathode i.e. the point where the sample was loaded. This peak corresponded to ^{99m}Tc -RH. The second peak, obtained at a distance of 3.0 ± 0.5 cm from the cathode corresponded to ^{99m}Tc -resveratrol, the third peak at 10 ± 1.0 cm, corresponded to $^{99m}\text{TcO}_4^-$ and a fourth, unknown peak was obtained at 5 ± 0.6 cm.

In vitro stability

Radiochemical purity of ^{99m}Tc -resveratrol, determined as described above, was used as a measure to assess the stability of the complex at different physiological conditions.

At fixed concentrations of resveratrol (624 μM), and $\text{SnCl}_2 \cdot 2\text{H}_2\text{O}$ (632 μM) as well as fixed radioactivity of $^{99m}\text{TcO}_4^-$ activity (3.7MBq), the radiochemical yield of ^{99m}Tc -resveratrol was recorded at regular time intervals from 0-120 min. As shown in Figure 3a, the highest yield of $88.2 \pm 1.1\%$ was achieved after 30 min of incubation at room temperature. Saturation in yield was achieved thereafter as no increase was observed with further increase in incubation time.

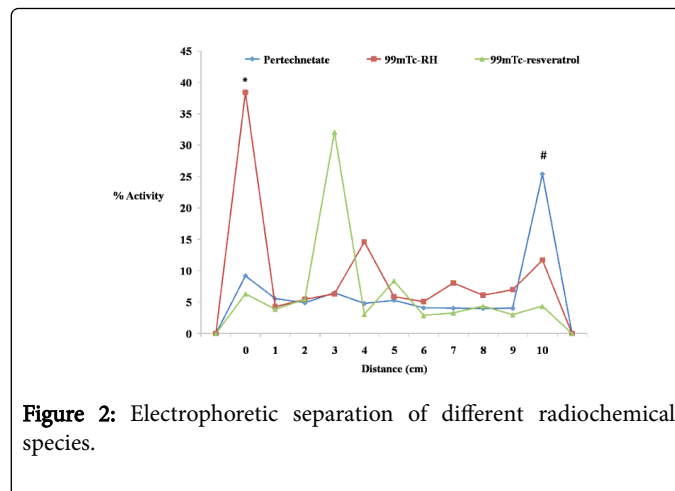


Figure 2: Electrophoretic separation of different radiochemical species.

Electrophoretogram shows peaks corresponding to the migration distances travelled by the ^{99m}Tc -complexes towards the anode on Whatman paper strips. $^{99m}\text{TcO}_4^-$ and ^{99m}Tc -RH colloids (as reference compounds) were also run simultaneously along with ^{99m}Tc -resveratrol. Experiment was run with samples in triplicate and repeated 2 times. Migration distances for all radiochemical species were compared with that of ^{99m}Tc -Resveratrol. * $p \leq 0.05$, † $p \leq 0.01$, # $p \leq 0.001$ by one way ANOVA.

Labeling efficiency of ^{99m}Tc -resveratrol which was observed to be $>85\%$, was found to be sufficiently stable for 2 hours at room temperature in normal saline and for 3 hours in serum (Figure 3b). Also, as shown in Figure 3c, the radio-complex was found to be stable over a wide pH range, with maximum% labelling efficiency values, observed between pH 5-7.

Cytotoxicity

Trypan blue staining

Staining of non-viable cells using trypan blue stain (Figure 4a) was used to measure the *in vitro* cytotoxicity of ^{99m}Tc -resveratrol over a range of different concentrations, when incubated with HT 29 colon cancer cells. Percentage cell viability was comparable to control values (100 %) for all concentrations up to 20 μM . However, increasing the concentration further decreased the cell viability to around 60% at 160 μM of ^{99m}Tc -resveratrol.

MTT assay

Absorbance values for metabolized products of MTT by viable cells were used to determine the *in vitro* cytotoxicity for a range of different concentrations of ^{99m}Tc -resveratrol incubated with HT 29 colon cancer cells. As shown in Figure 4b, the percentage viability varied between 64 to 90% up to 20 μM compared to control values (100%) and then decreased below 65% at concentrations higher than 20 μM .

Blood haemolysis assay

As shown in Figure 4c, increase in blood haemolysis was observed on increasing the concentration of ^{99m}Tc -resveratrol to 400 μM . However, the values were markedly lower as compared to values obtained with 1% Triton X 100. Further, the values were comparable to control (blank) levels for concentrations up to 26 μM but increased significantly thereafter ($p \leq 0.001$).

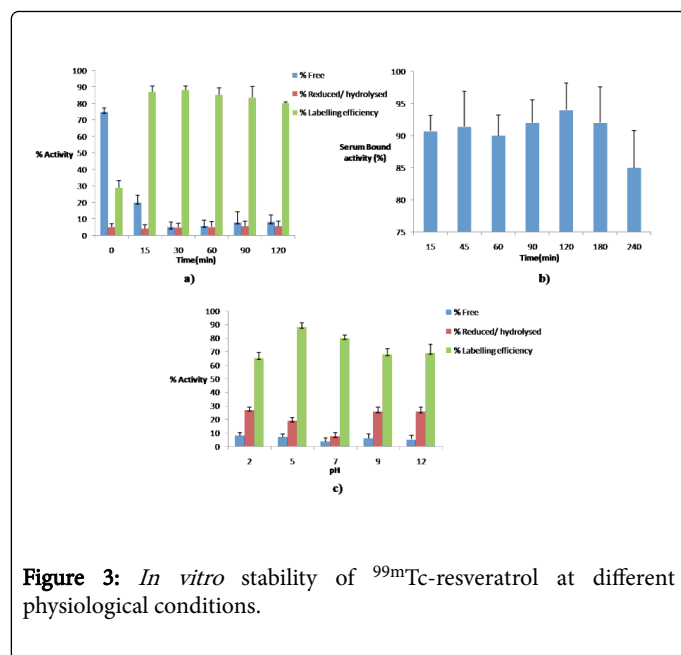


Figure 3: *In vitro* stability of ^{99m}Tc-resveratrol at different physiological conditions.

Percentage bound activity values as a function of time represent the stability of the radio-complex with time a) in saline b) in serum and c) at different pH. Experiment was run with samples in triplicate and repeated 2 times.

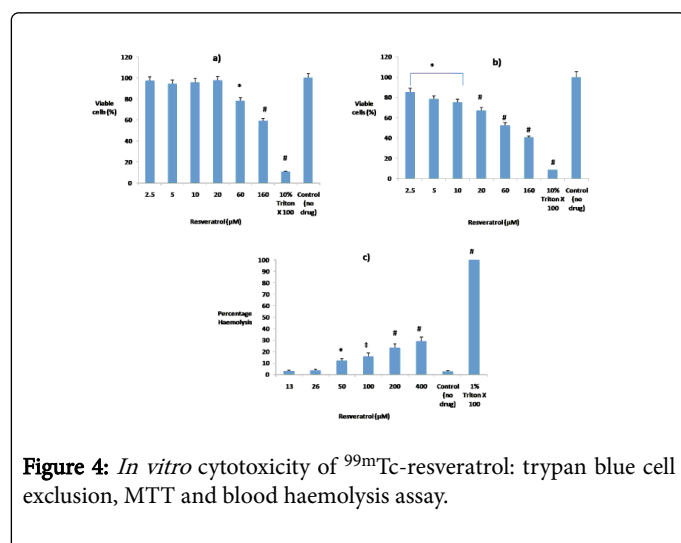


Figure 4: *In vitro* cytotoxicity of ^{99m}Tc-resveratrol: trypan blue cell exclusion, MTT and blood haemolysis assay.

In vitro cytotoxicity (24 hours) at different concentrations of ^{99m}Tc-resveratrol as evaluated by a) Trypan blue, b) MTT, c) blood haemolysis assay. Experiment was run with samples in triplicate and repeated 2 times. Values at various concentrations were compared to control values. * $p \leq 0.05$, † $p \leq 0.01$, # $p \leq 0.001$ by one way ANOVA, when compared to values of control.

Total cell binding

The cell bound fraction at various concentrations of ^{99m}Tc-resveratrol, ranged between 1.5-3.5% of total added amount. Further, the amount of ^{99m}Tc-resveratrol bound to the cells increased with increase in concentration of ^{99m}Tc-resveratrol (since the fraction of total added amount of ^{99m}Tc-resveratrol bound to the cells remained

unchanged with increasing concentration of ^{99m}Tc-resveratrol) (Figure 5a). Also, as shown in Figure 5b, a significant increase in cell bound ^{99m}Tc-resveratrol was noticed with increase in the incubation time. When compared to values at 0.25 hours, significant increase in cell binding was noticed at 1, 2 and 4 hours ($p \leq 0.001$).

Internalization and sub-cellular fraction binding of ^{99m}Tc-resveratrol in HT 29 cells

It can be observed that for each concentration of ^{99m}Tc-resveratrol, maximum internalization was obtained after 2 hours after which the internalization decreased. As shown in Figure 6, a maximum uptake of 15-23 % of total cell bound ^{99m}Tc-resveratrol was observed with 40 μ M at 2 hours. Decrease in internalization was observed with concentration above 40 μ M and after 2 hours of incubation.

Figure 7 shows binding of ^{99m}Tc-resveratrol to different cellular fractions of HT 29 following incubation at 37°C for 2 hours with increasing concentrations of ^{99m}Tc-resveratrol. The study was performed to determine the cellular fraction (s) enriched in binding sites for the radio-complex. Radioactivity associated with each fraction represented the percentage of total internalized radio-complex bound to the respective cell fraction. The results suggest that an appreciable percentage of internalized ^{99m}Tc-resveratrol was bound to soluble cytosolic proteins and free membranes, whereas binding to nuclear and large cellular components was much lower. Further, on increasing the amount of ^{99m}Tc-resveratrol, binding to cytosolic fraction, which comprised of soluble proteins and free membranes increased, whereas the binding decreased in case of other cell fractions.

Saturation binding

Out of the three subcellular cell fractions, saturation binding characteristics were observed only with the cytosolic fractions. The radioactivity measured in cytosolic fractions was found to be reduced in the presence of unlabeled resveratrol when compared to samples, in which unlabeled resveratrol was not present (Figure 8a). Analysis of saturation binding data by Graph pad prism 6.05 software revealed binding sites with β max of 72.63nM/106 cells and an apparent affinity (Kd) of 24.24 μ M (Figure 8b).

Mechanism of cell internalization

Internalization of ^{99m}Tc-resveratrol in cancer cells, in our study, occurred both via active and passive processes but predominantly by passive process, especially at low concentrations of ^{99m}Tc-resveratrol (Figure 9). Internalization at high concentrations was equally contributed by both active and passive processes. Furthermore, as the incubation time was increased from 1-4 hours, cell internalization via active process increased, whereas passive internalization decreased to finally attain similar values at 4 hours.

To further characterize internalization via active process, cells were pre-incubated with endocytosis inhibitors at 37°C, before incubation with ^{99m}Tc-resveratrol (Figure 10). Since, maximum cell internalization was observed after 2 hours, as observed from previous experiments, characterization of active internalization of ^{99m}Tc-resveratrol using metabolic inhibitors was carried out after 2 hours of incubation. When the cells were energy deprived by pre-incubation at 37°C in a medium containing 0.1% sodium azide [17], a marked decrease in the extent of internalization was observed when compared to control samples. Significant decrease in internalization as compared to control samples was observed when cells were preincubated with

cytochalasin B and colchicin ($p \leq 0.001$), inhibitors of macropinocytosis [18], and general pinocytosis respectively, and also with chlorpromazine [19] which is an inhibitor of clatherin mediated endocytosis processes [20] but to a lesser extent ($p \leq 0.01$).

Discussion

Radiochemical purity

Maximum labelling yield of $89.4 \pm 0.35\%$ was obtained on incubating $624 \mu\text{M}$ each of trans-resveratrol and stannous chloride with 3.7MBq ($100 \mu\text{Ci}$) of $^{99m}\text{TcO}_4^-$ activity for 30 min at room temperature and at physiological pH (5-7). Increasing the amount of $\text{SnCl}_2 \cdot 2\text{H}_2\text{O}$ or trans-resveratrol beyond $632 \mu\text{M}$ decreased the radiochemical purity by increasing the colloidal fraction in the formulation. Whereas, excess of $\text{SnCl}_2 \cdot 2\text{H}_2\text{O}$ is known to form insoluble colloids that can co-precipitate with reduced $^{99m}\text{TcO}_4^-$ thereby reducing the labelling efficiency [16], colloid formation with excess of resveratrol could be related to low solubility of the compound in aqueous medium that may have increased precipitation or colloid formation. Saturation in yield after 30 min of incubation at room temperature indicated 30 min as the minimum reaction time required to radiolabel resveratrol with ^{99m}Tc successfully. Further, as no change in labelling yield was observed upto 2 hours, the shelf life of 2 hours was obtained for the radio-complex. This means that the synthesized radio-complex could be used best within 2 hours after preparation without compromising on its radiochemical purity.

Paper electrophoresis

Depending on their electrophoretic mobility, each charged complex (free $^{99m}\text{TcO}_4^-$, ^{99m}Tc -RH, and ^{99m}Tc -resveratrol) travelled a specific distance on the Whatman paper strip, as depicted in Figure 2. The unknown peak at 5 ± 0.6 cm from the point of application towards the anode possibly belonged to oxo groups of ^{99m}Tc (TcO_3^+ , $\text{trans-}^{99m}\text{TcO}_2^+$, $\text{Tc}_2\text{O}_3^{4+}$) i.e. cores of reduced ^{99m}Tc , that were not bound to resveratrol or probably were detached from resveratrol due to strong electric field forces. A decrease in migration velocity associated with increase in molecular radius (at equal net charge) has been observed for oxobis (dithiolato) technetate (V) anions [TcOL_4]-L stands for ligands containing thiol groups) whose electrophoretic migration was found to be approximately one third that of $^{99m}\text{TcO}_4^-$ [21], thus indicating that the peak obtained at ~ 3 cm from cathode could be that of oxo core containing complex, ^{99m}Tc -resveratrol.

In vitro stability

Stability in serum for 3 hours can be observed as an important finding with regard to the *in vivo* application of ^{99m}Tc -resveratrol, since the complex can be retained in its non-dissociated form in the circulation over a long time and therefore can be efficiently transported to various body organs via systemic blood circulation without dissociating into its chemical constituents. Further, the radiochemical purity of ^{99m}Tc -resveratrol which was observed to be $>85\%$ was found to be sufficiently stable for 2 hours at room temperature in normal saline which suggests that the radio-complex can be used for various *in vitro* and *in vivo* applications even after 2 hours from the time of synthesis.

Although the radio-complex was found to be stable over a wide pH range, maximum labeling efficiency was observed between pH 5-7. Increasing or decreasing the pH above or below this range probably

caused particle aggregation leading to the formation of colloidal impurities in the formulation [16].

Cytotoxicity

MTT is a water soluble tetrazolium salt, which is converted to an insoluble purple formazan by cleavage of the tetrazolium ring by succinate dehydrogenase within the mitochondria. The formazan product is impermeable to the cell membranes and therefore it accumulates in healthy cells and thus is informative of cell death due to mitochondrial damage. On the other hand, trypan blue staining has a more general action ranging from a generic damage of cell membrane and is therefore, used to check plasma membrane integrity. Trypan blue can stain only dead cells as it can easily cross the damaged plasma membrane in these cells.

After 24 hours of treatment with ^{99m}Tc -resveratrol, the cells showed excellent viability up to $20 \mu\text{M}$ concentration of ^{99m}Tc -resveratrol as demonstrated by both, MTT and trypan blue exclusion assay (Figure 4a and 4b). The results clearly indicate that ^{99m}Tc -resveratrol was mildly toxic to cancer cells up to $20 \mu\text{M}$ concentration. Cytotoxic parameters, for unlabeled resveratrol using cancer cell lines, have been reported previously [22,23]. According to Kocsis et al., 2005, [22] no cytotoxic effects were observed with $100 \mu\text{M}$ of trans-resveratrol when MCF-7 human mammary carcinoma cells were incubated with different concentrations of trans-resveratrol for 24 hours.

Blood haemolysis observed after 24 hours of incubation with red blood cells also revealed mild toxic effects of ^{99m}Tc -resveratrol on RBCs, as the percentage haemolysis values for concentration upto $26 \mu\text{M}$ did not vary much from control (blank) values (Figure 4c). 2% haemolysis was observed for control and 3-4 % for concentrations up to $26 \mu\text{M}$ of ^{99m}Tc -resveratrol. At concentrations above $26 \mu\text{M}$, haemolysis increased upto 30% as can be observed from the Figure 4c. According to previous reports, resveratrol showed no haemolytic effect on human red blood cells up to $100 \mu\text{g/ml}$ ($438 \mu\text{M}$) [24]. Therefore, the cytotoxicity observed for ^{99m}Tc -resveratrol at concentrations higher than $26 \mu\text{M}$ could be attributed to the radionuclide (^{99m}Tc) complexed with trans-resveratrol.

Thus, the results from cytotoxicity assays indicate that the synthesized radiopharmaceutical has negligible cytotoxicity upto concentrations $20 \mu\text{M}$ which indicates that it has potential for *in vivo* applications.

Cancer cell binding and internalization of ^{99m}Tc -resveratrol

On analysing the data on total cell bound ^{99m}Tc -resveratrol (Figure 5), the amount of ^{99m}Tc -resveratrol bound to the cells, seemed to increase both with increase in concentration and with increase in incubation time upto 2 hours.

Cancer cell (HT 29 colon cancer) binding at 37°C a) after 2 hours, as a function of increasing concentration of ^{99m}Tc -resveratrol and b) as a function of incubation time. Experiment was run with samples in triplicate and repeated 2 times.

Similarly, cell internalization also increased with increase in the amount of ^{99m}Tc -resveratrol incubated with the cells and with increase in incubation time, however a decrease in the cellular internalization was observed after 2 hours at concentrations higher than $40 \mu\text{M}$ of ^{99m}Tc -resveratrol (Figure 6).

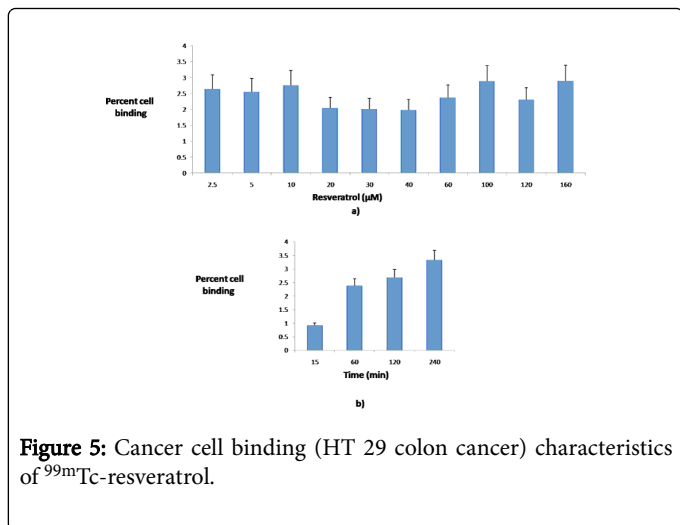


Figure 5: Cancer cell binding (HT 29 colon cancer) characteristics of ^{99m}Tc -resveratrol.

On increasing the incubation time above 2 hours or the concentration above 40 μM , the internalization would decrease appreciably. Therefore, for maximum cell internalization *in vivo*, cancer cells would require at least 2 hour contact time with approximately 40 μM ^{99m}Tc -resveratrol.

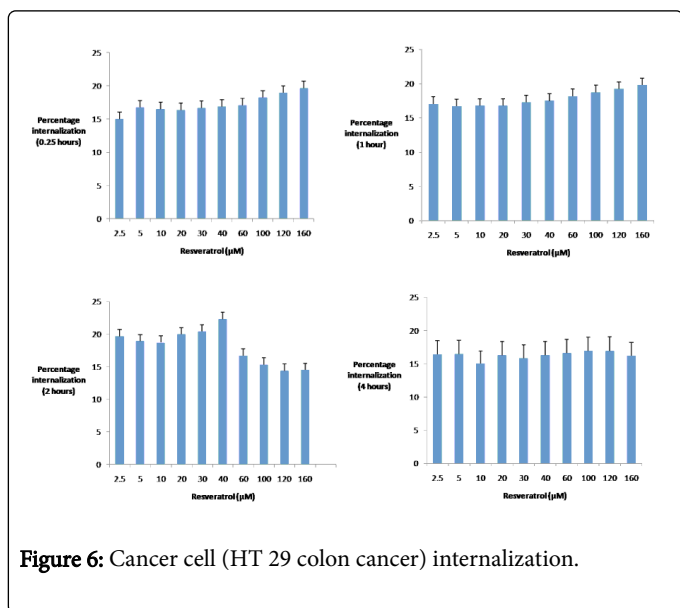


Figure 6: Cancer cell (HT 29 colon cancer) internalization.

Cellular internalization as a percentage of total cell bound ^{99m}Tc -resveratrol. Internalization was observed at different time points (0.25 to 4 hours) with increasing concentrations of ^{99m}Tc -resveratrol (2.5 μM to 160 μM) incubated with the cells. Experiment was run with samples in triplicate and repeated 2 times.

Cell fraction and saturation binding study

Binding of ^{99m}Tc -resveratrol to various cellular fractions was studied following incubation at 37°C for 2 hours (Figure 7). A large fraction of the internalized ^{99m}Tc -resveratrol was bound to cytosolic fraction of cancer cells, which consisted of the soluble cytosolic proteins and free membranes, whereas binding to nuclear fraction and large cellular components was much lower.

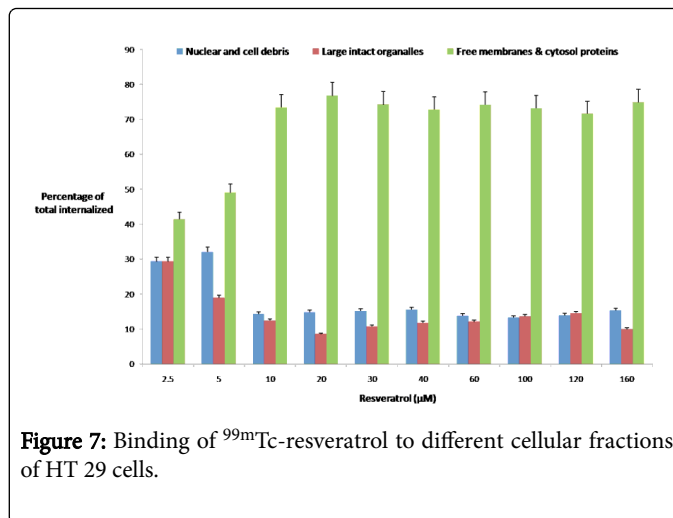


Figure 7: Binding of ^{99m}Tc -resveratrol to different cellular fractions of HT 29 cells.

Bars and error bars represent mean \pm S.D. values for subcellular fraction binding of ^{99m}Tc -resveratrol represented as percentage of total internalized radio-complex after 2 hours of incubation with HT 29 colon cancer cells. Cells were incubated with increasing concentrations (2.5-160 μM) of ^{99m}Tc -resveratrol at 37°C. Experiment was run with samples in triplicate and repeated 2 times.

Further, the presence of unlabeled resveratrol along with ^{99m}Tc -resveratrol decreased the binding of ^{99m}Tc -resveratrol to cytosolic fractions, which suggests that the binding sites for ^{99m}Tc -resveratrol that were similar to native unlabeled trans-resveratrol (Figure 8) were concentrated either on free membranes or soluble cytosolic proteins. Binding studies have been carried out in rat brain homogenates, using tritium labelled resveratrol ($[3\text{H}]\text{-resveratrol}$) previously by Han et al., 2006 [16] to identify binding sites for unlabeled resveratrol in different subcellular fractions. According to his study, saturable specific binding sites for $[3\text{H}]\text{-resveratrol}$ were identified in the plasma membrane fractions. The results obtained in our study are in line with these reports, since maximum binding for ^{99m}Tc -resveratrol was obtained in the cytosolic fraction which, in addition to soluble cytosolic proteins, also contained free membranes including plasma membrane. Further the binding sites observed in our study were similar to those of native resveratrol i.e. binding sites specific to resveratrol, as observed by Han et al., 2006 [16], using $[3\text{H}]\text{-resveratrol}$. Saturation binding experiments in our study reports a maximum number density value (β max) for the binding sites as 72.63 nM/106 cells, and an apparent affinity (Kd) of ^{99m}Tc -resveratrol for these sites as 24.24 μM .

Mechanism of internalization

Cells have mechanisms for the rapid movement of ions and solute molecules across the plasma membrane. These mechanisms are of two types: passive transport, which requires no direct expenditure of metabolic energy, and active transport, which uses metabolic energy to move solutes across the plasma membrane. Lipophilic substances enter cell membranes by passive diffusion or passive transport (carrier) and hydrophilic by passive transport (e.g. ion channels) or active transport [25].

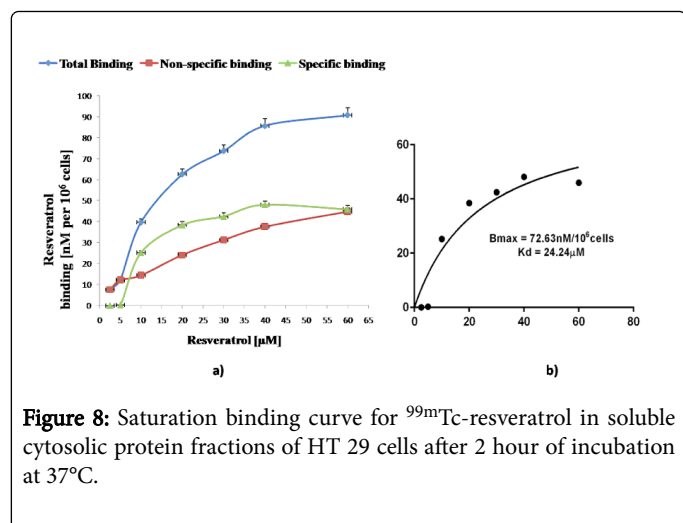


Figure 8: Saturation binding curve for ^{99m}Tc -resveratrol in soluble cytosolic protein fractions of HT 29 cells after 2 hour of incubation at 37°C.

a) Binding experiments were performed in the presence or the absence of 100 mM unlabelled resveratrol; specific (triangular points) binding represents the difference between total (diamond shaped points) and non-specific (square points) binding. Total binding, non-specific binding and specific binding for ^{99m}Tc -resveratrol is expressed as mean \pm S.D values for nM of ^{99m}Tc -resveratrol bound per 10⁶ cells. b) Binding parameters (β_{max} and K_d) as analysed using Graph pad prism 6.05 software. Experiment was run with samples in triplicate and repeated 2 times.

Most nano scale macromolecules and molecular assemblies are internalized through endocytosis, an active uptake process in which macromolecules are in fluxed into cells after being enclosing within membrane vesicles upon contact with the cell membrane. According to reports, trans-resveratrol, which is lypophilic in nature, can enter the cells both by active and passive modes. Whereas, passive internalization for trans-resveratrol has been reported to occur through passive diffusion and a carrier-facilitated passive transport, active transport has been reported to occur via receptor mediated endocytosis [26,27]. After initial insertion in the outer plasma membrane lipid bilayer, resveratrol accumulates in lipid rafts, and is taken up by lipid raft dependent, clathrin-independent endocytosis [28].

In order to study the uptake mechanism for ^{99m}Tc -resveratrol the first step was to determine whether active or passive processes are involved in its uptake. In order to confirm the involvement of active process, the cells were energy depleted using sodium azide prior to ^{99m}Tc -resveratrol exposure. Sodium azide is known to inhibit the respiratory chain in the mitochondria, thus impairing the production of ATP in the cell and consequently the active uptake [29]. The principle being that, if the general internalization mechanism for ^{99m}Tc -resveratrol by cancer cells involved only active processes, there would be no uptake of ^{99m}Tc -resveratrol by the cells following pretreatment with sodium azide, since the energy mediated processes would be inhibited by the pretreatment. In case any uptake was observed, it would be due to passive transport. Energy dependence/ independence for ^{99m}Tc -resveratrol internalization was further studied by incubating the cells with ^{99m}Tc -resveratrol at 4°C. Since incubation at 4°C inhibits active processes, as several proteins and enzymes are sensitive to temperature [14,15] the total uptake obtained at 4°C would correspond to passive uptake only.

When the total uptake measured at 37°C was corrected for passive uptake measured at 4°C, the curve obtained corresponded to active transport (Figure 9). Cell internalization of ^{99m}Tc -resveratrol occurred both via active and passive processes but predominantly by passive process especially at low concentrations of ^{99m}Tc -resveratrol. Internalization at high concentrations was equally contributed by active and passive processes. Furthermore, transition from passive to active mode could be observed as the incubation time was increased from 1-4 hours. With increase in incubation time, cell internalization via active process increased, whereas internalization via passive process decreased. Internalization via active uptake observed at higher concentrations and after long incubation time, suggested that initially the radio-complex is internalized passively into the cells, but later, in addition to passive mode, active mode is also adopted, in order to internalize more of the radio-complex into the cells.

Mechanism of cancer cell internalization (Active/Passive) for ^{99m}Tc -resveratrol. Percent cell internalization (fraction of total cell bound activity) at 4°C and 37°C was expressed as mean \pm S.D. values for different concentrations of ^{99m}Tc -resveratrol at different time points (0.25 hours to 4 hours). Experiment was run with samples in triplicate and repeated 2 times.

Energy depletion with sodium azide, also inhibited the internalization, confirming the involvement of active process during internalization of ^{99m}Tc -resveratrol by cancer cells. Thus, both active and passive internalization modes were observed for ^{99m}Tc -resveratrol in the present study. Several other studies also support our observation where both active and passive cell internalization for trans-resveratrol has been observed in various normal and cancer cell lines including human umbilical vein endothelial cells (HUVECs) [27], SW 480, SW 620, HT 29, HCT 116 human colon carcinoma cells, human leukemic monocyte lymphoma U937 cells, rat non-transformed small intestinal IEC-18 cells [28] and Hep G2 cell line, derived from a human hepatoblastoma [26].

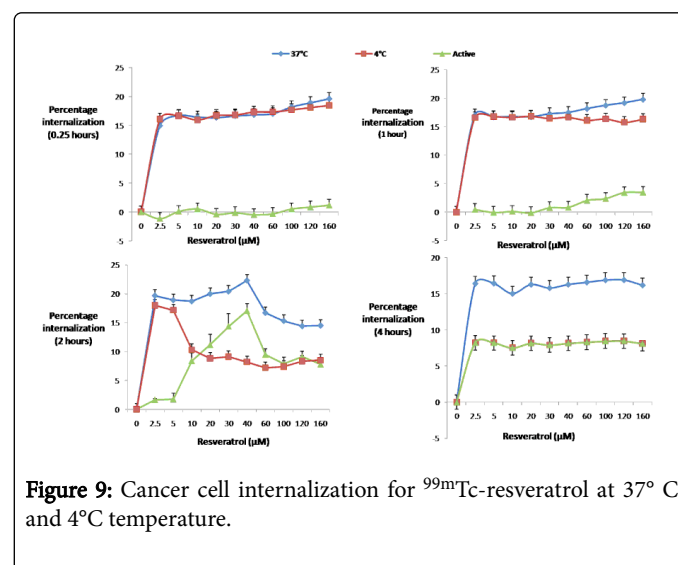


Figure 9: Cancer cell internalization for ^{99m}Tc -resveratrol at 37°C and 4°C temperature.

As discussed above, ^{99m}Tc -resveratrol uptake is partly due to an active process. In order to study which endocytic mechanism is implied, cells were treated with inhibitors for various energy dependent endocytic pathways (Figure 10) cytochalasin B for macropinocytosis, colchicin for general pinocytosis and chlorpromazine for clathrin dependent endocytosis. Cells were

treated with inhibitors at non cytotoxic concentrations, as determined by trypan blue staining of the cells treated with inhibitors. Uptake of ^{99m}Tc-resveratrol was inhibited maximally by macropinocytosis inhibitor cytochalasin B indicating macropinocytosis as the primary mechanism for active uptake of ^{99m}Tc-resveratrol by cancer cells. Previously reported uptake mechanisms for trans-resveratrol using [3H]-resveratrol, indicate pinocytosis (clathrin-independent endocytosis) as the internalization mechanism for resveratrol [28]. The difference in the endocytic mechanism responsible for the uptake of [3H]-resveratrol and ^{99m}Tc-resveratrol could be attributed to the difference in the particle size. Molecular assemblies and particles >1 μm in size are internalized by macropinocytosis, whereas particles in nm range are internalized by receptor mediated endocytosis [30].

This suggests that particle size of ^{99m}Tc-resveratrol was either very large as compared to [3H]-resveratrol or, it formed molecular clusters. As increase in molecular size from nanometer to micrometer for the same molecule (resveratrol) in similar experimental conditions is not possible, formation of molecular clusters of ^{99m}Tc-resveratrol was presumably the reason for change in the active internalization process.

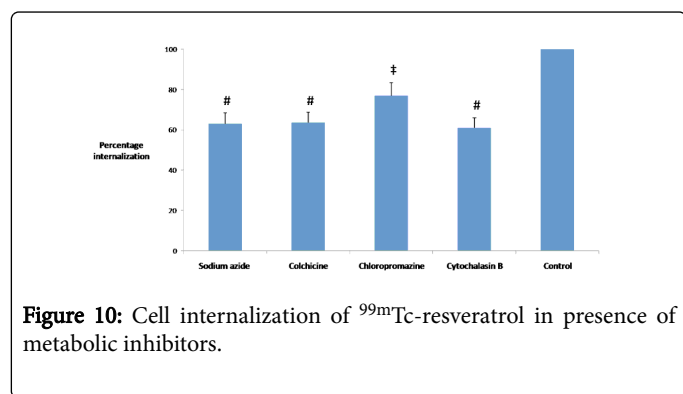


Figure 10: Cell internalization of ^{99m}Tc-resveratrol in presence of metabolic inhibitors.

Mean ± S.D. values for percentage internalization of ^{99m}Tc-resveratrol (10 μM after 2 hours of incubation with HT 29 cells) following pre-incubation with metabolic inhibitors. Experiment was run with samples in triplicate and repeated 2 times. Statistical evaluation was done using One way ANOVA. *p≤0.05, ‡p≤0.01, #p≤0.001 by one way ANOVA, when compared to values of control.

Conclusion

The present study optimizes and characterizes the radiolabeling of resveratrol with ^{99m}Tc. Further, the preliminary evaluation of ^{99m}Tc-resveratrol in targeting cancer cells using *in vitro* investigations, demonstrates common binding sites for ^{99m}Tc-resveratrol and unlabeled resveratrol in the cytosolic fractions of cancer cells. With the data available it is difficult to conclude whether a single class of binding sites or multiple binding sites with similar binding affinity contributed towards the specific binding of ^{99m}Tc-resveratrol to its targets but it is possible to conclude that the binding targets were similar to that of native resveratrol. Studies are in progress to identify the cytosolic sites to which the complex apparently binds the chemical structure of the radio-complex, and bio-distribution characteristics *in vivo* using animal colon cancer models.

Acknowledgement

The authors would like to thank Post Graduate Institute for Medical Education and Research (PGIMER) Chandigarh, India for providing

necessary material and equipment for the study. The financial support by the Department of Science and Technology (DST), New Delhi is gratefully acknowledged.

References

1. Zhou JH, Cheng HY, Yu ZQ, He DW, Pan Z, et al. (2011) Resveratrol induces apoptosis in pancreatic cancer cells. *Chin Med J (Engl)* 124: 1695-1699.
2. Pirola L, Frojdo S (2008) Resveratrol: one molecule, many targets. *IUBMB Life* 60: 323-332.
3. Zykova TA, Zhu F, Zhai X, Ma WY, Ermakova SP, et al. (2008) Resveratrol directly targets COX-2 to inhibit carcinogenesis. *Mol Carcinog* 47: 797-805.
4. Bakhle YS (2001) COX-2 and cancer: a new approach to an old problem. *Br J Pharmacol* 134: 1137-1150.
5. Gehm BD, Mc Andrews JM, Chien PY, Jameson JL (1997) Resveratrol, a polyphenolic compound found in grapes and wine, is an agonist for the estrogen receptor. *Proc Natl Acad Sci USA* 94:14138-14143.
6. Ashby J, Tinwell H, Pennie W, Brooks AN, Lefevre PA, et al. (1999) Partial and weak oestrogenicity of the red wine constituent resveratrol: consideration of its superagonist activity in MCF-7 cells and its suggested cardiovascular protective effects. *J Appl Toxicol* 19:39-45.
7. Bowers JL, Tyulmenkov VV, Jernigan SC, Klinge CM (2000) Resveratrol acts as a mixed agonist/antagonist for estrogen receptors alpha and beta. *Endocrinology* 141: 3657-3667.
8. Armstrong CM, Billimek AR, Allred KF, Sturino JM, Weeks BR, et al. (2013) A novel shift in estrogen receptor expression occurs as estradiol suppresses inflammation-associated colon tumor formation. *Endocr Relat Cancer* 20: 515-525.
9. Leav I, Lau KM, Adams JY, McNeal JE, Taplin ME, et al. (2001) Comparative studies of the estrogen receptors beta and alpha and the androgen receptor in normal human prostate glands, dysplasia, and in primary and metastatic carcinoma. *Am J Pathol* 159: 79-92.
10. Royuela M, de Miguel MP, Bethencourt FR, Sánchez-Chapado M, Fraile B, et al. (2001) Estrogen receptors alpha and beta in the normal, hyperplastic and carcinomatous human prostate. *J Endocrinol* 168: 447-454.
11. Mosmann T (1983) Rapid colorimetric assay for cellular growth and survival: application to proliferation and cytotoxicity assays. *J Immunol Methods* 65: 55-63.
12. Cotica LF, Freitas VF, Dias GS, Santos IA, Vendrame SC, et al. (2012) Simple and facile approach to synthesize magnetite nanoparticles and assessment of their effects on blood cells. *J Magn Magn Mater* 324: 559-563.
13. Han YS, Bastianetto S, Dumont Y, Quirion R (2006) Specific plasma membrane binding sites for polyphenols, including resveratrol, in the rat brain. *J Pharmacol Exp Ther* 318: 238-245.
14. Iacopetta BJ, Morgan EH (1983) The kinetics of transferrin endocytosis and iron uptake from transferrin in rabbit reticulocytes. *J Biol Chem* 258: 9108-9115.
15. Saraste J, Palade GE, Farquhar MG (1986) Temperature-sensitive steps in the transport of secretory proteins through the Golgi complex in exocrine pancreatic cells. *Proc Natl Acad Sci U S A* 83: 6425-6429.
16. Saha GB (1996) *The Chemistry of Tc-99m-Labeled Radiopharmaceuticals*. 5:1 Albuquerque, New Mexico.
17. Gao H, Yang Z, Zhang S, Cao S, Shen S, et al. (2013) Ligand modified nanoparticles increases cell uptake, alters endocytosis and elevates glioma distribution and internalization. *Sci Rep* 3: 2534.
18. Goldman R (1976) The effect of cytochalasin B and colchicine on concanavalin A induced vacuolation in mouse peritoneal macrophages. *Exp Cell Res* 99: 385-394.
19. Xin H, Jiang X, Gu J, Sha X, Chen L, et al. (2011) Angiopep-conjugated poly(ethylene glycol)-co-poly(ε-caprolactone) nanoparticles as dual-

- targeting drug delivery system for brain glioma. *Biomaterials* 32: 4293-4305.
20. Nam HY, Kwon SM, Chung H, Lee SY, Kwon SH, et al. (2009) Cellular uptake mechanism and intracellular fate of hydrophobically modified glycol chitosan nanoparticles. *J Control Release* 135: 259-267.
 21. Byrne EF, Smith JE (1979) Technetium complexes of aliphatic thiols. Synthesis and characterization of oxobis (1,2- and 1,3-dithiolato) technetium (V) anions. *Inorg Chem* 18: 1832-1835.
 22. Kocsis Z, Marcsek ZL, Jakab MG, Szende B, Tompa A (2005) Chemopreventive properties of trans-resveratrol against the cytotoxicity of chloroacetanilide herbicides in vitro. *Int J Hyg Environ Health* 208: 211-218.
 23. Berardi V, Ricci F, Castelli M, Galati G, Risuleo G (2009) Resveratrol exhibits a strong cytotoxic activity in cultured cells and has an antiviral action against polyomavirus: potential clinical use. *J Exp Clin Canc Res* 28:96.
 24. Jung HJ, Seu YB, Lee DG (2007) Candidicidal action of resveratrol isolated from grapes on human pathogenic yeast *C. albicans*. *J Microbiol Biotechnol* 17: 1324-1329.
 25. Efferth T (2006) *Molekulare Pharmakologie and Toxikologie*. Springer Verlag, Heidelberg.
 26. Lançon A, Delmas D, Osman H, Thénot JP, Jannin B, et al. (2004) Human hepatic cell uptake of resveratrol: involvement of both passive diffusion and carrier-mediated process. *Biochem Biophys Res Commun* 316: 1132-1137.
 27. Chen D, Zhao H, Feng YE (2013) The expression of cell adhesion molecules in colorectal cancer tissue and its clinical values. *Turk J Med Sci* 43: 946-950.
 28. Colin D, Limagne E, Jeanningros S, Jacquelin A, Lizard G, et al. (2011) Endocytosis of resveratrol via lipid rafts and activation of downstream signaling pathways in cancer cells. *Cancer Prev Res (Phila)* 4: 1095-1106.
 29. Tsubaki M (1993) Fourier-transform infrared study of azide binding to the Fea3-CuB binuclear site of bovine heart cytochrome c oxidase: new evidence for a redox-linked conformational change at the binuclear site. *Biochemistry* 32: 174-182.
 30. Verma A, Stellacci F (2010) Effect of surface properties on nanoparticle-cell interactions. *Small* 6: 12-21.